

First results studying the transmutation of ^{129}I , ^{237}Np , ^{238}Pu , and ^{239}Pu in the irradiation of an extended $^{\text{nat}}\text{U}/\text{Pb}$ -assembly with 2.52 GeV deuterons*

M. I. Krivopustov,^{1**} A. V. Pavliouk,¹ A. D. Kovalenko,¹ I. I. Mariin,¹

A. F. Elishev,¹ J. Adam,¹ A. Kovalik,¹ Yu. A. Batusov,¹ V. G. Kalinnikov,¹ V. B. Brudanin,¹ P. Chaloun,¹
 V. M. Tsoupko-Sitnikov,¹ A. A. Solnyshkin,¹ V. I. Stegailov,¹ Sh. Gerbish,¹ O. Svoboda,² Z. Dubnicka,²
 M. Kala,² M. Kloc,² A. Krasa,² A. Kugler,² M. Majerle,² V. Wagner,² R. Brandt,³ W. Westmeier,^{3,4}
 H. Robotham,⁴ K. Siemon,⁴ M. Bielewicz,⁵ S. Kilim,⁵ M. Szuta,⁵ E. Strugalska-Gola,⁵ A. Wojeciechowski,⁵
 S. R. Hashemi-Nezhad,⁶ M. Manolopoulou,⁷ M. Fragopolou,⁷ S. Stoulos,⁷ M. Zamani-Valasiadou,⁷ S. Jokic,⁸
 K. Katovsky,⁹ O. Schastny,⁹ I. V. Zhuk,¹⁰ A. S. Potapenko,¹⁰ A. A. Safronova,¹⁰ Zh. A. Lukashevich,¹⁰
 V. A. Voronko,¹¹ V. V. Sotnikov,¹¹ V. V. Sidorenko,¹¹ W. Ensinger,¹² H. D. Severin,¹² S. Batsev,¹³
 L. Kostov,¹³ Kh. Protokhrstov,¹³ Ch. Stoyanov,¹³ O. Yordanov,¹³ P. K. Zhivkov,¹³ A. V. Kumar,¹⁴
 M. Sharma,¹⁴ A. M. Khilmanovich,¹⁵ B. A. Marcinkevich,¹⁵ S. V. Korneev,¹⁵ Ts. Damdinsuren,¹⁶
 Ts. Togoo,¹⁶ H. Kumawat,¹⁷ Collaboration “Energy plus Transmutation”

¹ Joint Institute for Nuclear Research, Joliot-Curie 6, 141980 Dubna, Russia

² Nuclear Physics Institute, Řež near Praha, Czech Republic

³ Kernchemie, Chemistry Department, Philipps-University, 35032 Marburg, Germany

⁴ Dr. Westmeier GmbH, 35085 Ebsdorfergrund, Germany

⁵ Institute of Atomic Energy, 05-400 Otwock-Swierk near Warsaw, Poland

⁶ School of Physics, A28, University of Sydney, NSW 2006, Australia

⁷ School of Physics, Aristotle University, Thessaloniki 54124, Greece

⁸ Vinca Institute of Nuclear Science, Belgrad, Serbia

⁹ Czech Technical University, Praha, Czech Republic

¹⁰ Joint Institute of Power and Nuclear Research, Sosny, 220109 Minsk, Belarus

¹¹ Kharkov Institute of Physics and Technology, Kharkov, Ukraine

¹² Analytical Chemistry, FB 11, Technical University, 64287 Darmstadt, Germany

¹³ Institute of Nuclear Research and Nuclear Energy, Sofia, Bulgaria

¹⁴ University of Rajasthan, Jaipur, India

¹⁵ Stepanov Institute of Physics, Minsk, Belarus

¹⁶ National University, Ulaanbaatar, Mongolia

¹⁷ Bhabha Atomic Research Center, Mumbai 400085, India
 Collaboration “Energy plus Transmutation”

(Received June 9, 2008)

An extended U/Pb-assembly was irradiated with an extracted beam of 2.52 GeV deuterons from the Nuclotron accelerator of the Laboratory of High Energies within the JINR in Dubna, Russia. The lay-out of this experiment and first results are reported. The Pb-target (diameter 8.4 cm, length 45.6 cm) is surrounded by a $^{\text{nat}}\text{U}$ -blanket (206.4 kg) and used for transmutation studies of hermetically sealed radioactive samples of ^{129}I , ^{237}Np , ^{238}Pu and ^{239}Pu . Estimates of transmutation rates were obtained as result of measurements of gamma-activities of the samples. Information about the spatial and energy distribution of neutrons in the volume of the lead target and the uranium blanket was obtained with sets of activation threshold detectors (Al, Y and Au) and solid state nuclear track detectors (SSNTD). An electronic ^3He neutron detector was tested on-line. A comparison of experimental data with theoretical model calculations using the MCNPX program was performed yielding satisfactory results.

Introduction

The technology of accelerator-driven-systems (ADS) is part of world-wide attempts to enable CO_2 -free generation of energy, together with simultaneous attempts to solve the problem of the final deposition of long-lived radioactive waste. The Laboratory of High Energies (LHE) with its accelerator Nuclotron within the Joint Institute of Nuclear Research (JINR) in Dubna, Russia is engaged in this research activity with a project called “Energy plus Transmutation”.¹ The central

experimental part is a massive lead target surrounded by a uranium blanket (U/Pb-assembly), as described by KRIVOPUSTOV et al.^{1,2} It was irradiated with extracted proton beams with energies from 0.7 to 2.0 GeV for transmutation studies of radioactive samples of ^{129}I , ^{237}Np , ^{238}Pu , ^{241}Am and ^{239}Pu .^{2,3} A variety of different experimental techniques was employed, such as classical radiochemical measurements, solid state nuclear track detectors (SSNTD), nuclear emulsions and uranium fission calorimeters.^{2–11} BALDIN et al.,¹² MALAKHOV et al.¹³ and KOVALENKO et al.¹⁴ described these activities within the broader frame of the research goals of the JINR. This topic of ADS has also been studied by

* This work is dedicated to the cherished memory of Professor Vladimir Pavlovich Pereygin from the JINR in Dubna, Russia.

** E-mail: krivopustov@lhe.jinr.ru

other groups; some of their results can be found elsewhere.^{15–20} TOLSTOV et al.²¹ and VASSIL'KOV et al.²² irradiated extended lead targets with protons, deuterons and heavier ions.

This paper describes the first experiment using a deuteron beam in our system:

The production of secondary neutrons by protons is compared to the production by deuterons having about the same kinetic energy of 2.52 GeV.

The list of radioactive samples was extended over earlier transmutation studies and includes now: ^{129}I , ^{237}Np , ^{238}Pu and ^{239}Pu .

A ^3He electronic counter was tested for the first time for on-line neutron counting during the irradiation.

Experimental

General experimental setup

The major apparatus of the “Energy plus Transmutation” project is schematically shown in Fig. 1. The detailed technical design was carried out by the All-Russian Institute of Nuclear Energy Machine Building (VNIAEM) in Moscow and the steel structure was manufactured at the mechanical workshop of the Laboratory of High Energies JINR.

The experimental setup consists of the following parts:

The lead target is divided into four sections (diameter of 8.4 cm and total length of 45.6 cm; weight of 28.6 kg).

The uranium blanket is divided into four sections; each section consists of 30 fuel rods of natural uranium inside an aluminum cover (36 mm diameter, 104 mm length, weight of 1.72 kg). Each section contains 51.6 kg of uranium, so the whole blanket contains 206.4 kg of natural uranium.

Beam monitoring devices and various activation experiments. This includes radiochemical targets, solid state nuclear track detectors (SSNTD)s, proportional ionization chambers and Polaroid films.

A ^3He detector system for on-line neutron counting with automatic movement within the experimental area was installed. The present experiment was the first one to test the ^3He detector in “electronuclear” investigations. The detector can determine the spatial density and energy distributions of the neutron flux.

The top view onto the uranium blanket is shown in Fig. 2. One can identify the 4 sections of the U-blanket. The small gaps between the sections and the front end as well as the back end of the U-blanket contain five polyethylene plates where activation detectors and SSNTDs are fixed to study the neutron spectra and the particle fluence around the four sections of the lead target.

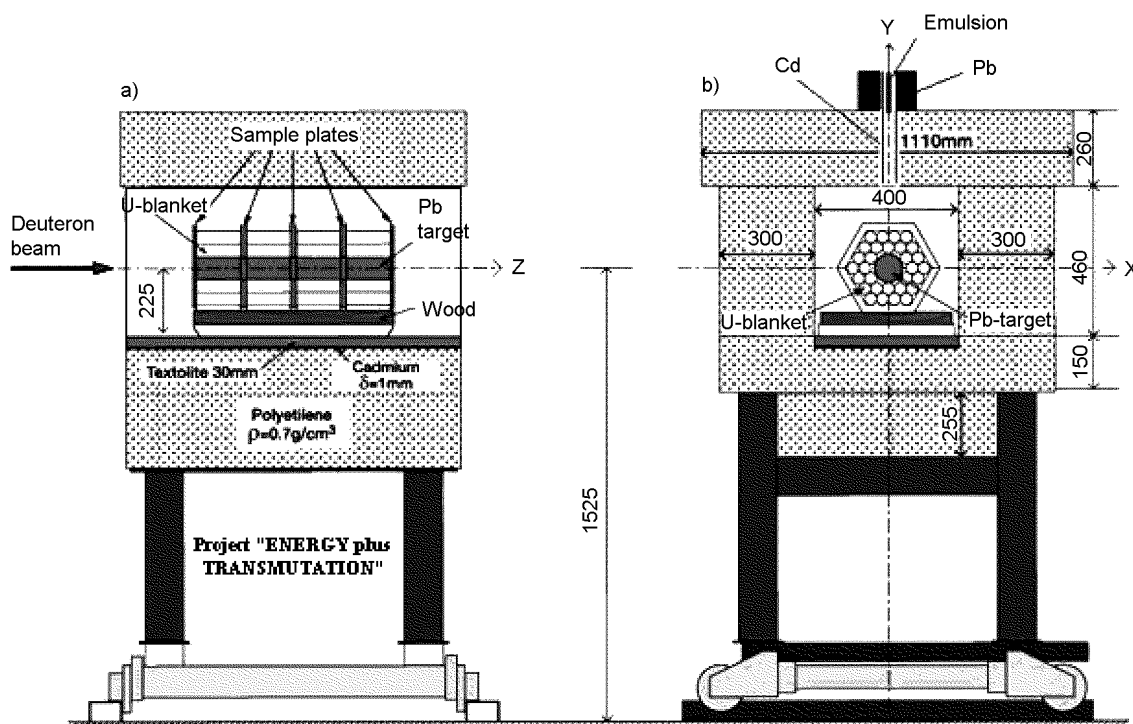


Fig. 1. The U/Pb-assembly is inside of a massive shielding and placed onto a mobile platform, which can be moved into and out of the beam line. Fig. a (YZ cross section) gives a cut through the assembly along the beam line, Fig. b (XY cross section) shows a cut through the assembly perpendicular to the beam line in the position between the first and the second section of the U/Pb-assembly. Nuclear emulsions are mounted over the hole on the top of the shielding in order to measure spectra from very fast neutrons

A plate for fixation of radioactive samples and other small detectors is mounted on top of the second section of the blanket (counting from the left side in Fig. 2). The radioactive samples ^{129}I , ^{237}Np , ^{238}Pu and ^{239}Pu are the circular cups seen in Fig. 2. These highly radioactive targets are hermetically sealed inside aluminum containers (Fig. 3).

The wooden shielding box around the Pb/U-assembly itself (Fig. 1) is filled with granulated polyethylene containing boron carbide and it has a 1 mm cadmium cover on the inner side. The biological shield box has dimensions of $100 \times 106 \times 111 \text{ cm}^3$ and its weight is 950 kg. It is moved into the irradiation position at focus F3N of the Nuclotron experimental site using a special rail system.

Five sets of nuclear emulsion for neutron energy measurements through proton recoil are placed on top of the biological shielding, as indicated in Fig. 1b. Results of an earlier application of this nuclear emulsions technique for investigation of neutron spectra have been published.⁴

The transmutation samples (^{129}I , ^{237}Np , ^{238}Pu and ^{239}Pu) were placed on top of the second section of the uranium blanket (Fig. 2) and fixed on a 1 mm thick plastic holder-plate of $104 \times 140 \text{ mm}^2$ size. In each experiment one sample of each isotope was used plus one sample of stable ^{127}I , as the radioactive ^{129}I sample contains 15% of ^{127}I . The ^{238}Pu sample is also not pure but it contains other plutonium isotopes, mainly ^{239}Pu (16.75%). Radioactive materials are encapsulated in an aluminum holder (a special duralumin alloy) with diameter of 34 mm (Fig. 3). Some properties of the radioactive samples used are given in Table 1.

The radioactive samples were manufactured by collaboration of three Russian nuclear research institutes: the Leipunski Institute of Physics and Power Engineering at Obninsk, the Bochvar All-Russian Institute of Inorganic Materials at Moscow (VNIINM), and the "Mayak" Plant at Ozersk (Chelyabinsk region). Samples are regularly tested for being hermetically sealed, and in addition especially before and after irradiations for alpha- and beta-activity on their surfaces.

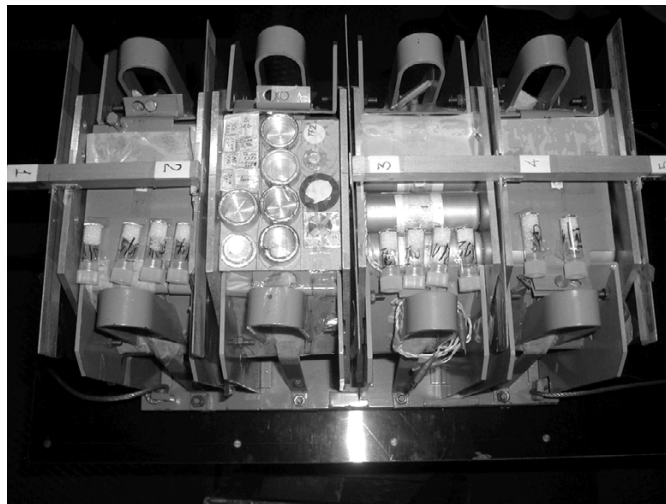


Fig. 2. Photo of the four U-blanket section (top view). The three gaps between the blanket sections as well as the front and the back ends are locations for detector plates (Numbers 1, 2, 3, 4 and 5) to measure particle fluence inside and around the U/Pb-assembly. On the top surface of the blanket additional activation detectors and radioactive waste samples (^{129}I , ^{237}Np , ^{238}Pu and ^{239}Pu) are placed for transmutation studies

Table 1. Basic properties of radioactive samples for transmutation studies. Half-lives are taken from Reference 36

Sample	Decay type	Half-life, y	Weight, g	Isotopes, %	
I-129	β^-	$1.57 \cdot 10^7$	0.591	85	I-129
				0.121	15
Np-237	α	$2.14 \cdot 10^6$	1.085	~100	Np-237
Pu-238	α	87.74	0.0477	72.92	Pu-238
				16.75	Pu-239
				2.87	Pu-240
				0.35	Pu-241
				0.11	Pu-242
				Rest is unknown	
Pu-239	α	$2.411 \cdot 10^4$	0.455	~100	Pu-239

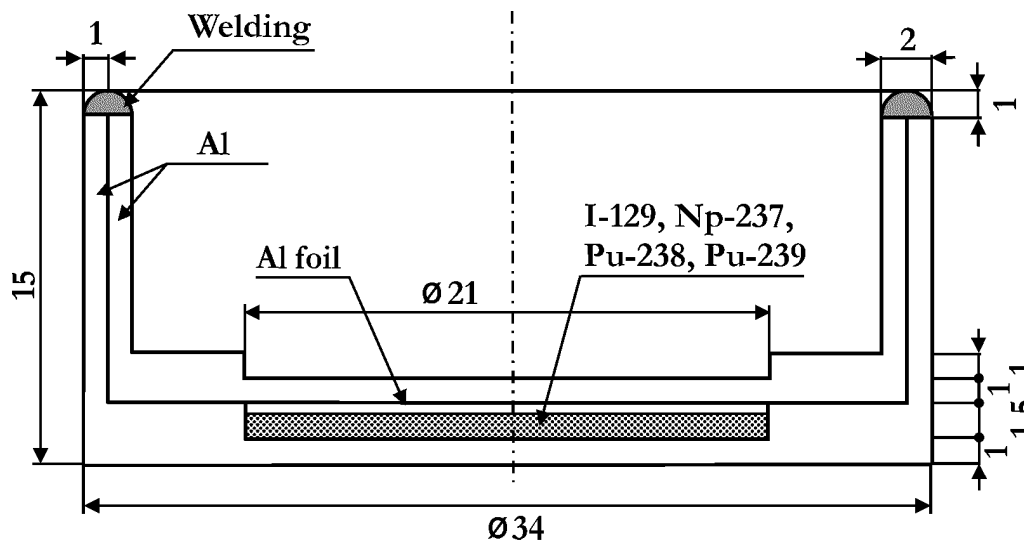


Fig. 3. Technical drawing of the weld-sealed aluminum container for radioactive samples (^{129}I , ^{237}Np , ^{238}Pu and ^{239}Pu). Dimensions are in mm

Activation and SSNT-detectors, nuclear emulsions and samples of various technological materials

The neutron field in various locations was measured with neutron activation threshold detectors as Al, Ti, V, Mn, Fe, Co, Ni, Cu, Y, Nb, In, Dy, Lu, W, Au and Bi foils placed onto the top of the second section of the U-blanket (Fig. 2).

Neutron distributions were studied along the surface of the U-blanket and on the top of the shielding using SSNT-detectors. CR39 foils acting as particle detectors were placed parallel to the target axis. One part of the detector was in contact with a neutron converter (Kodak LR115, type 2B, containing $\text{Li}_2\text{B}_4\text{O}_7$). This converter provides information about the neutron fluence, detecting the alpha-particle tracks in CR39 produced by $^{10}\text{B}(n,\alpha)^7\text{Li}$ and $^6\text{Li}(n,\alpha)^3\text{H}$ reactions. Another part of CR39 in contact with the neutron converter was covered in addition on both sides with 1 mm thick Cd foils. In this way epithermal neutrons could be measured without interference from thermal neutrons.

The thermal neutron component (up to about 1 eV) was determined by subtracting the measured track density of the Cd-covered from the uncovered region of the CR39 detector. Fast neutrons were determined by proton recoil tracks on the CR39 detector itself (elastic scattering of neutrons on H atoms of the detector).²³ The neutron detectable energy region covered by these proton recoils is between 0.3 MeV and 3 MeV.²⁴ SSNTDs were also used as fission detectors. Evaporation of approximately $100 \mu\text{g}/\text{cm}^2$ of ^{235}U or ^{232}Th on Makrofol E detector foils provided samples to study the thermal (up to about 1 eV with ^{235}U target) and fast neutron (above 2 MeV with ^{232}Th target) distributions along the U-blanket.²³

The same SSNTDs were used also for monitoring the high-energy neutron field between the U-blanket sections.

The spectra of very fast neutrons ($E > 10$ MeV) leaving the U/Pb-assembly³ were measured with highly sensitive thick nuclear emulsions G-5BR (baseless, relativistic) with dimensions of $100 \times 25 \times 1.2 \text{ mm}^3$. These emulsions were placed on the outer upper surface of the top shielding of the U/Pb-assembly as shown in Fig. 1b.

^3He neutron counter

The basic characteristics of the ^3He proportional counter are summarized in Table 2. The electronic measurement system is straightforward and consists of a high voltage power supply, a preamplifier (Canberra, Model 2006), an amplifier (Tennelec Model TC205), and a computer based multi-channel analyzer (Tennelec PCA III). The ^3He counter was manufactured by LND Inc., New York, USA.

The system was calibrated using the Tandem, Van de Graaff Accelerator Facility at the Institute of Nuclear Physics, NCSR Demokritos, Athens, Greece.²⁵ The detector was irradiated with mono-energetic neutrons in the energy range of $230 \text{ keV} \leq E_n \leq 7.7 \text{ MeV}$, produced via $^7\text{Li}(p,n)^7\text{Be}$ and $^2\text{H}(d,n)^3\text{He}$ reactions. Due to the high pressure and its large dimensions the ^3He counter could be used effectively for measuring neutron energies up to about 7 MeV.

A linear response with incident neutron energy was observed for neutron energies up to 7 MeV, both for the full energy peak and the recoil peak. The energy resolution varied from 11% for thermal neutrons down to 4% for higher energies.

The disadvantage of ^3He counters is their relatively large dead time of several tens of μs which restricts the use in high intensity neutron fields. In order to avoid space charge effects or even paralyzing of the detector, the maximum count rate must be kept well below 10^4 cps. In this irradiation the motorized stage, which was specifically designed for holding and moving the counter during the experiment, was positioned to the maximum possible distance at about 4.7 m away from the center of U-blanket (Fig. 4). The cylindrical wall of the counter was covered with 1.2 mm Cd to minimize the contribution of the scattered thermal neutrons, coming mainly from the concrete walls.

Gamma-spectra measurement

The gamma-counting of activation threshold detectors, Al and Cu beam monitors, and transmutation samples ^{129}I , ^{237}Np , ^{238}Pu and ^{239}Pu was carried out with HPGe gamma-ray spectrometers with resolution below 1.80 keV for the 1332 keV gamma-line. The systems were provided by Dzhelepov Laboratory of Nuclear Problems of JINR. Different geometrical

positions as well as various filters composed of Cu, Cd and Pb were used depending on the activities of the samples. Spectra measurements started few hours after the end of the irradiation and lasted for up to two weeks. The HPGe detector systems were calibrated using ^{57}Co , ^{60}Co , ^{88}Y , ^{137}Cs , ^{152}Eu , ^{154}Eu and ^{228}Th (and daughters products) and ^{133}Ba sources which provide several gamma-lines ranging from 80 up to 2614 keV.

The gamma-spectra were analyzed and the net peak areas were calculated using the DEIMOS program.²⁶ All necessary corrections for coincidences and background contributions were done. About five hundred gamma-ray spectra were measured and analyzed.

Beam monitoring

The beam intensity profile during the Nuclotron irradiation is shown in Fig. 5. The deuteron irradiation lasted for 7 hours and 59 minutes. The beam geometry and the total beam fluence reaching the actual U/Pb-target were measured separately by two independent beam monitors.

Table 2. Basic characteristics of the ^3He counter

Detector gas	Pressure, atm	Gas contents, %		Cathode:	Anode:	Effective length, cm	Effective diameter, cm
		^3He	Kr	material, thickness	material, diameter, mm		
^3He	6	^3He 64.7	Kr 33.3	Stainless steel 304, 0.089 cm	Tungsten, 0.025	15	5
		CO_2 2.0					

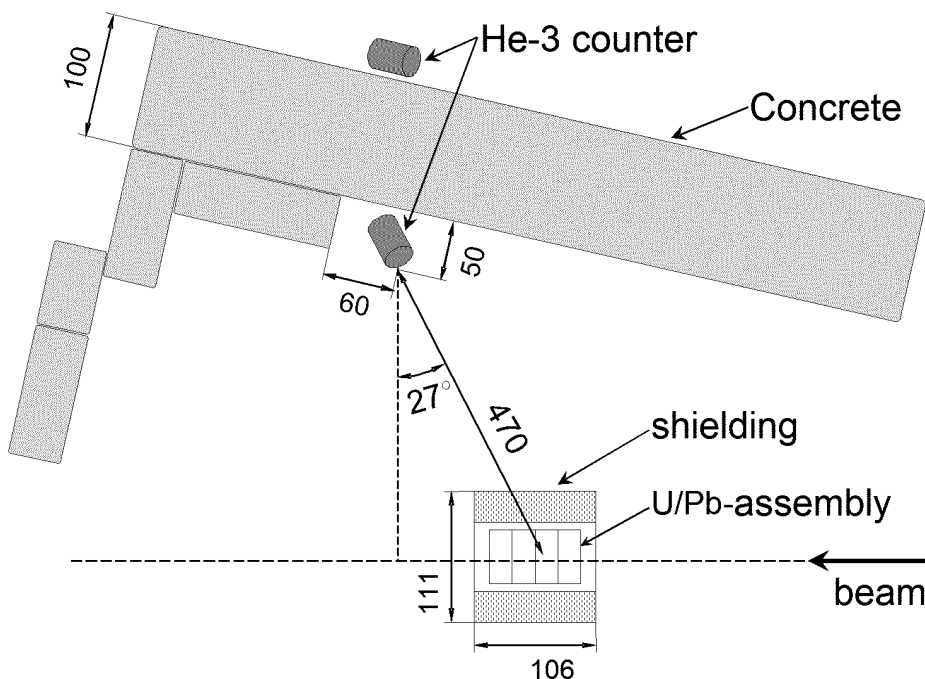


Fig. 4. Positioning of the ^3He counter with respect to the beam direction and U/Pb-assembly. The distances are given in cm

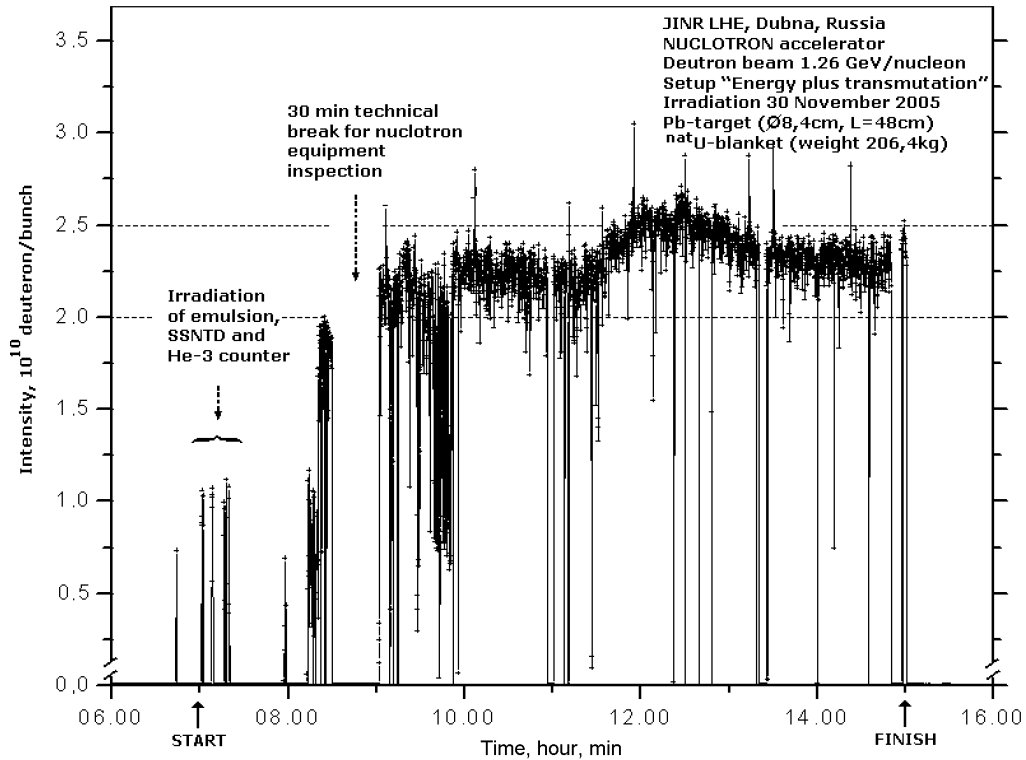


Fig. 5. The intensity profile of the 2.52 GeV deuteron beam on the Pb-target with U-blanket as a function of time

The beam position was first determined before the major irradiation. One accelerator burst of deuterons was sent onto Polaroid films (placed in front of the target) in order to check the shape, location, and alignment of the beam. The final beam was centered in front of the target, went parallel through the target axis, and had an elliptical shape close to a circle with half-axes of not more than 1 cm.

Two sets of monitor foils were used to measure the beam profile during the irradiation.

Aluminum and copper foils used as radiochemical beam monitors: The total beam intensity was determined by the standard activation analysis method using thin foils of Al. The nuclear reaction was $^{27}\text{Al}(d,3p2n)^{24}\text{Na}$. The yield of β^- radioactive nucleus ^{24}Na was determined with the help of γ -spectrometry. For deuterium there is only one value available in the literature of the cross section for the $^{27}\text{Al}(d,3p2n)^{24}\text{Na}$ reaction, i.e., at 2.33 GeV²⁷ kinetic energy. The published data were re-evaluated giving a cross section value of:

$$\sigma_{2.33 \text{ GeV}}(^{27}\text{Al}(d,3p2n)^{24}\text{Na})=15.38\pm 1.12 \text{ mb} \quad (1)$$

As the excitation function is almost constant in this energy region, we have used the cross sections for 2.33 GeV also at 2.52 GeV.

There were two sets of Al-foils placed at 100 cm in front of the lead target, a distance which is sufficient to

suppress the influence of fast neutrons from the target, which could induce the competitive reaction $^{27}\text{Al}(n,\alpha)^{24}\text{Na}$.

The first set of $10\times 10 \text{ cm}^2$ Al-foils had a thickness of 250 μm . Using the cross section data from Eq. (1), the value of the integral deuteron flux determined from this Al-foil is $I_d=(6.42\pm 0.17)\cdot 10^{12}$ (statistical uncertainty only).

The second set was a circular ^{27}Al -foil with a thickness of 30 μm cut into an inner circle with diameter of 21 mm and four concentric rings with external diameters of 80, 90, 120 and 160 mm (Table 3). The integral deuteron flux determined from this Al-foil is $I_d=(6.50\pm 0.21)\cdot 10^{12}$ (statistical uncertainty only).

The weighted average of the integral deuteron flux was $I_d=(6.45\pm 0.13)\cdot 10^{12}$.

One $6\times 6 \text{ cm}^2$ Cu-foil with a thickness of 100 μm was placed closely in front of the target. After the irradiation, this foil was cut into nine pieces and each of these $2\times 2 \text{ cm}^2$ foils was measured and analyzed separately. Many products of $^{\text{nat}}\text{Cu}(d,X)$ -reactions were measured and the following isotopes were identified: ^{24}Na , ^{43}K , $^{48,44\text{m}}\text{Sc}$, ^{48}V , ^{48}Cr , ^{52}Mn , $^{58,56,55}\text{Co}$, ^{57}Ni and ^{61}Cu . As there are no available experimental cross sections for (d+Cu)-reactions, only the yields in different foils were compared. We found that the deuteron beam at the entrance to the target was shifted down by $\sim 1 \text{ mm}$ and to the right by $\sim 10 \text{ mm}$.

Table 3. Activities in the circular ^{27}Al -foils and calculated beam intensities

Inner diameter, cm	Outer diameter, cm	^{24}Na activity, Bq	Statistical uncertainty, %	Beam intensity, $\times 10^9$ deuterons/cm 2
0.0	2.1	253	3	7.43
2.1	8.0	274	3	0.60
8.0	9.0	5	20	0.04
9.0	12.0	8	13	0.02
12.0	16.0	11	9	0.01

SSNTDs used as beam monitors: Solid state nuclear detectors (SSNTDs) were also used as beam monitors. The beam profile was determined through the measurement of the distribution of fission tracks induced in natural lead covering the track detector. Two lines of 19 lead samples each were placed in front of the target in perpendicular directions: from left to right side and from bottom to top. The experimental fission-track density was fitted by a Gaussian distribution. The fitting parameters showed a shift of the beam centre: 0.3 ± 0.2 cm down, 1.5 ± 0.2 cm to the right (the uncertainties are estimated from the inaccuracy of samples location). The elliptical shape of the beam had a major half-axis in vertical direction, $\text{FWHM}_{\text{VER}} = 1.63 \pm 0.20$ cm, and in horizontal direction, $\text{FWHM}_{\text{HOR}} = 1.56 \pm 0.20$ cm. These results agree well with the results of the first method of the beam measurement. About $(97 \pm 3)\%$ of the beam hit the Pb-target, as shown in Table 3.

Results

Transmutation of ^{129}I , ^{237}Np , ^{238}Pu and ^{239}Pu

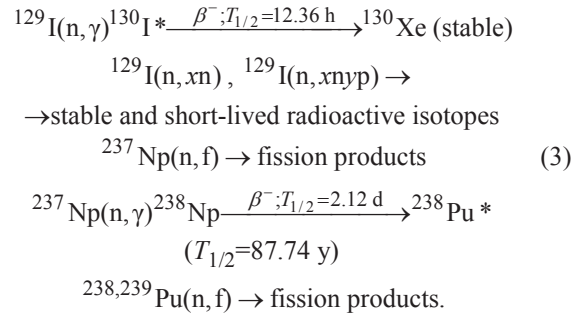
The experimental transmutation probabilities are expressed as “transmutation rate” $R(A_{\text{res}})$ or as “yield of residual nuclei” $B(A_{\text{res}})$, defined as follows:

$$\begin{aligned} R(A_{\text{res}}) &= \frac{N(A_{\text{res}})}{n_s \cdot I_D}, \\ B(A_{\text{res}}) &= \frac{N(A_{\text{res}})}{m_s \cdot I_D}, \\ R(A_{\text{res}}) &= B(A_{\text{res}}) \frac{A_s}{N_{\text{Avo}}} \end{aligned} \quad (2)$$

where $N(A_{\text{res}})$ is the number of atoms of product nuclei of mass A_{res} in a sample, n_s and m_s are the number of target atoms in the sample and its mass in grams, I_D is the deuteron fluence during irradiation; N_{Avo} is the Avogadro number, and A_s is the mass number of the sample nuclide.

Experimental transmutation yields, expressed as $B(A_{\text{res}})$, are ideal benchmark data to test theoretical models that describe the complex processes of interactions of the primary beam particles, the production of spallation neutrons, their secondary reactions in the U/Pb-assembly, particle transport

properties and finally the interaction with the sample. The correct description of all processes is an essential premise for credible results from the calculations that must be made in order to design a real transmutation setup on the technical or even industrial scale. The investigated nuclides are of particular importance as they are long-lived radioactive waste that could be transmuted with neutrons into stable or short-lived isotopes. This is an important radio-ecological aspect. The essential nuclear reactions are listed below [Eq. (3)]. The energy spectrum of neutrons in the U/Pb-assembly goes up to hundreds of MeV. Secondary neutrons are generated by the spallation reactions of 2.52 GeV deuterons in the lead target and also by fission reactions induced inside the sub-critical uranium blanket. Preliminary results for experimental transmutation rates from this deuteron experiment and a similar proton experiment are presented in Tables 4 and 5. Absolute reaction rates, $R(A_{\text{res}})$, are shown as this gives the number of product atoms produced per atom of the sample and per one incident deuteron or proton. Half-life data below are from Reference 36:



The irradiation of ^{127}I was used for consideration of a 15% contamination in the ^{129}I sample. The results are given in Table 4. Data from interactions of 2.0 GeV protons with the same targets are also presented.²⁸ The delay between the first γ -spectra measurement and end-of-irradiation (i.e., the cooling time) was 5 hours for proton and 11 hours for deuteron induced reactions. Thus, short-lived nuclei such as ^{128}I ($T_{1/2}=28$ min) could not be detected. It is seen from Table 4 that the results from deuterons of 2.52 GeV (present work) and protons of 2.0 GeV show remarkably similar yields with the exception of ^{126}I . This may indicate that the product cross sections are mainly determined by the total energy of the beams.

Table 4. Production rates $R(A_{res})$ observed in ^{127}I , ^{129}I and ^{237}Np samples, resulting from irradiations with proton and deuteron beams

Residual nucleus	$T_{1/2}$	Deuterons 2.52 GeV	Protons 2.0 GeV ²⁸
I-127 sample $\{R(A_{res}) \cdot 10^{29}\}$			
In-111	2.83 d	0.50(7)	0.38(10)
Te-119	16.05 h	1.15(18)	1.31(27)
Te-119m	4.69 d	1.15(26)	1.03(12)
I-121	2.12 h	3.87(100)	3.13(23)
Sb-122	2.70 d	1.24(15)	–
I-123	13.2 h	11.6(14)	13.0(10)
I-124	4.18 d	18.3(11)	19.0(10) a
Xe-125	16.9 h	20.1(86)	–
I-126	13.02 d	70.4(3)	81(4) 10
I-129 sample $\{R(A_{res}) \cdot 10^{29}\}$			
Te-121	16.8 d	4.93(94)	–
I-124	4.18 d	4.38(125)	4.0(5)
I-126	13.02 d	10.8(25)	22.5(44)
I-130	12.36 h	816(40)	809(33)
Np-237 sample $\{R(A_{res}) \cdot 10^{29}\}$			
Zr-97	17.0 h	0.188(29)	0.159(8)
Mo-99	2.75 d	1.64(47)	–
Te-132	3.26 d	0.217(32)	0.147(11)
I-133	20.8 h	0.265(75)	0.182(28)
Np-238	2.12 d	17.0(8)	13.3(3)

Table 5. Yields of product nuclei observed in ^{238}Pu and ^{239}Pu samples

Product nuclei	$T_{1/2}$	$B(\Delta B) \times 10^5$	$R(\Delta R) \times 10^{27}$
Pu-238 sample			
Zr-97	17.0 h	4.51(11)	15.6(4)
Xe-135	9.08 h	8.0(9)	29(4)
Pu-239 sample			
Sr-91	9.52 h	2.6(4)	10.3(17)
Zr-97	17.0 h	5.3(4)	20.9(17)
Ru-103	39.25 d	5.0(4)	19.8(17)
Sb-128	9.01 h	0.18(5)	0.72(22)
Te-132	3.26 d	4.3(4)	16.9(17)
I-133	20.8 h	6.8(7)	27(3)
I-135	6.61 h	4.6(8)	18(3)
Xe-135	9.08 h	3.0(8)	12(3)
Ba-140	12.75 d	5.2(6)	20.4(23)
Ce-143	33.04 h	3.6(4)	14.3(15)

For definition of B and R see Eq. (2), (ΔB) and (ΔR) are uncertainties.

Two plutonium isotopes (^{238}Pu and ^{239}Pu) were also irradiated and some product yields are given in Table 5. Due to the cooling time of 11 hours it was impossible to detect product isotopes with short half-lives. This is especially obvious for the 0.0477 g sample of ^{238}Pu where only two product nuclei could be identified.

Our investigations of transmutation of radioactive waste nuclides ^{129}I , ^{237}Np , ^{238}Pu and ^{239}Pu is in continuation of earlier work by this collaboration.^{10,11,28} Similar results in transmutation studies of ^{99}Tc and ^{129}I by other teams using different accelerators and setups have also been published, for example in References 19 and 29.

Results using ^{27}Al , ^{87}Y and ^{197}Au as activation and threshold detectors

The spatial and energy distributions of neutrons produced in the setup were studied with activation and threshold detectors in which the neutrons produced γ -emitting nuclides through (n, xn) , (n, α) and (n, γ) reactions. Different thresholds for various reactions allow probing the energy spectrum of neutrons. Foils of stable and mono-isotopic elements ^{27}Al , ^{89}Y and ^{197}Au were placed at different positions on top of the setup and also inside the lead target at longitudinal distances of 0 cm, 11.8 cm, 24.0 cm, 36.2 cm and 48.4 cm from the front of the Pb-target and at radial distances from 0.0 cm to 13.5 cm from the Pb-target axis between the four sections (Fig. 6).

After irradiation the activated foils were transported to the gamma-spectroscopy laboratory to investigate the activities with HPGe detectors. The decay rates of produced radioactive nuclides at the end-of-bombardment were converted into production rates $B(A_{res})$ defined in Eq. (2). The production rate $B(A_{res})$ is very sensitive to the energy threshold of the reaction and thus to the neutron spectrum at the foil position. The gamma-spectrum from each foil was measured twice.

When several gamma-ray line intensities of a radioactive nuclide could be measured the weighted average production rate $B(A_{res})$ was calculated for further analysis.

Radial production rate distributions $B(A_{res})$ for several isotopes produced in Au and Al activation detectors are shown in Figs 7–9, as examples. Figure 7 gives an example for a (n,γ) reaction due to low-energy neutrons: the resulting product distribution is rather homogeneous within the entire Pb-target and only slightly decreasing towards the rear end of the 48 cm long Pb-target. From Figs 8 and 9 one can see that the fluence of fast neutrons above 5 MeV is highest close to the axis of the Pb/U target system and decreasing in

radial direction (5 MeV is about the threshold for (n,xn) reactions).

Yttrium (^{89}Y) activation detectors had already been used in former experiments.³⁰ This time the sensors were placed on plastic foils in front of and between the four sections, as well as on the rear of the U/Pb-assembly in several positions at varying radial distances from the beam axis. Preliminary results presented give spatial distributions of ^{88}Y , ^{87}Y and ^{86}Y isotope production from (n,xn) reactions (Table 6 and Fig. 10).

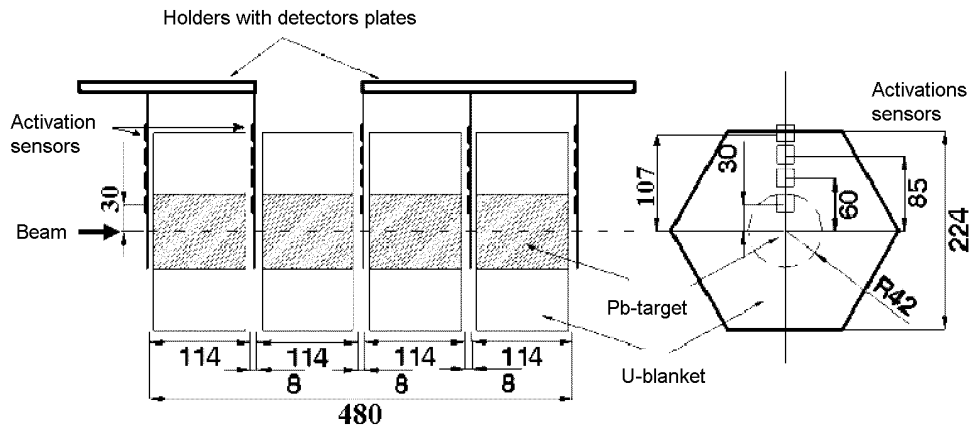


Fig. 6. Placement of activation sensors (see also Figs 1 and 2). The length of the U/Pb-assembly is 480 mm, the radial distance for activation sensors from the central axis extends up to 130 mm. The diameter of the activation samples is 10 mm

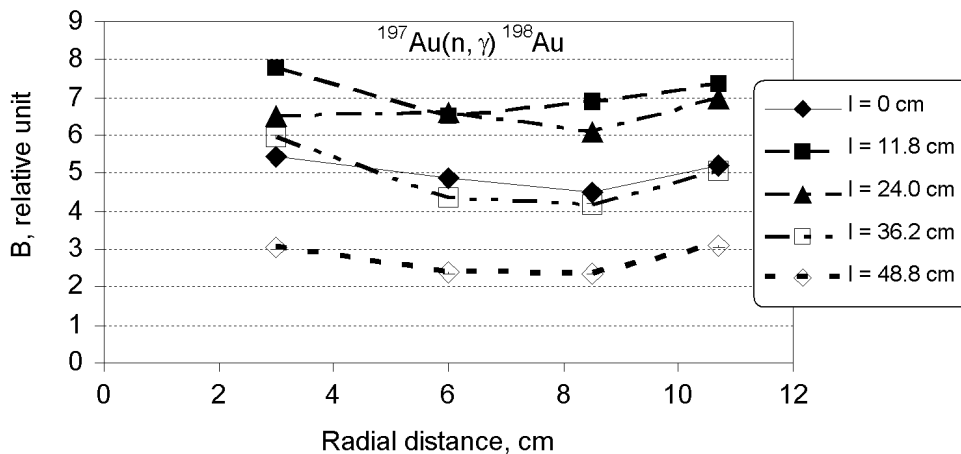


Fig. 7. Radial distributions of relative production rates $B(A_{res})$ for ^{198}Au produced in Au-foils by the non-threshold (n,γ) capture reaction measured for different distances from the front of the Pb-target. The lines are drawn to guide the eyes

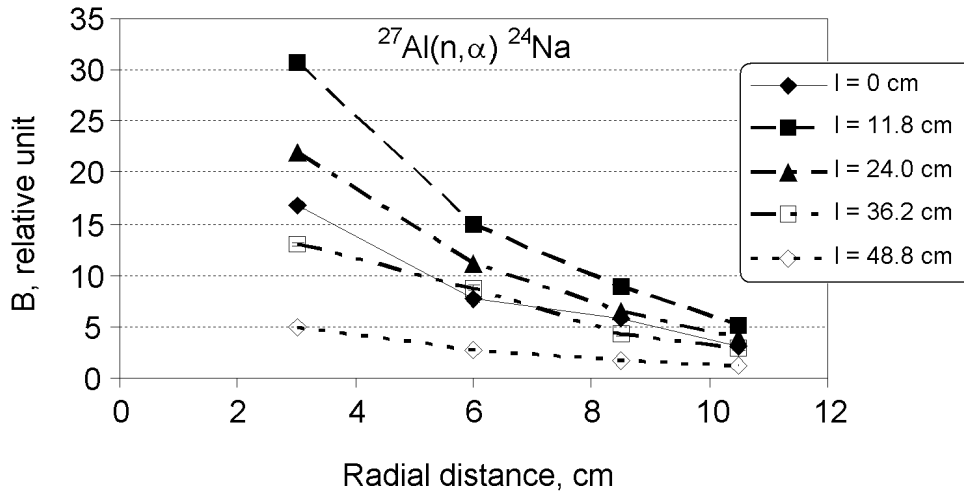


Fig. 8. Radial distributions of B -values $B(A_{res})$ for isotope ^{24}Na produced in Al-foils by (n, α) reaction with a threshold energy of 5.5 MeV. Distributions are shown for different distances from the front of the Pb-target. Lines are drawn to guide the eyes

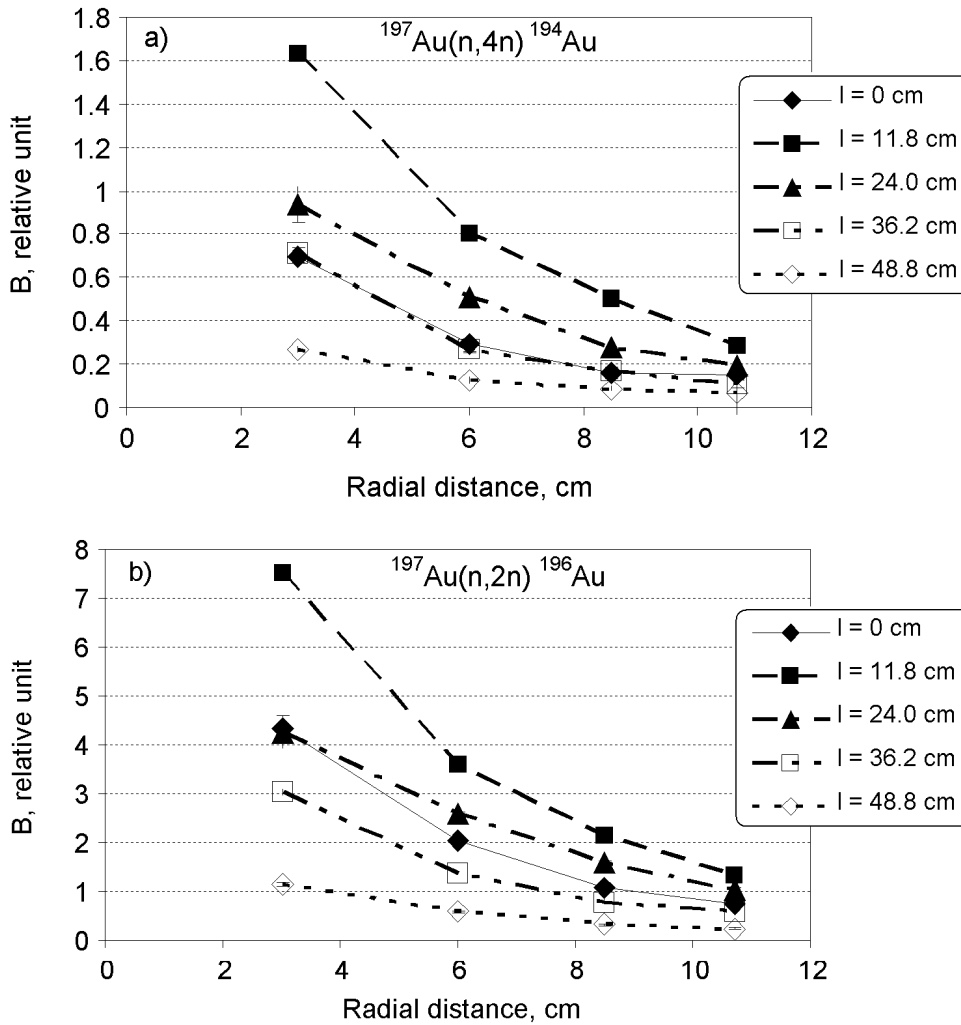


Fig. 9. Radial distributions of B -values $B(A_{res})$ for ^{196}Au (a) and ^{194}Au (b) isotopes produced in Au foils by $(n, 2n)$ and $(n, 4n)$ reactions with threshold energies of 8.1 MeV and 23.2 MeV, respectively. The lines are drawn to guide the eyes

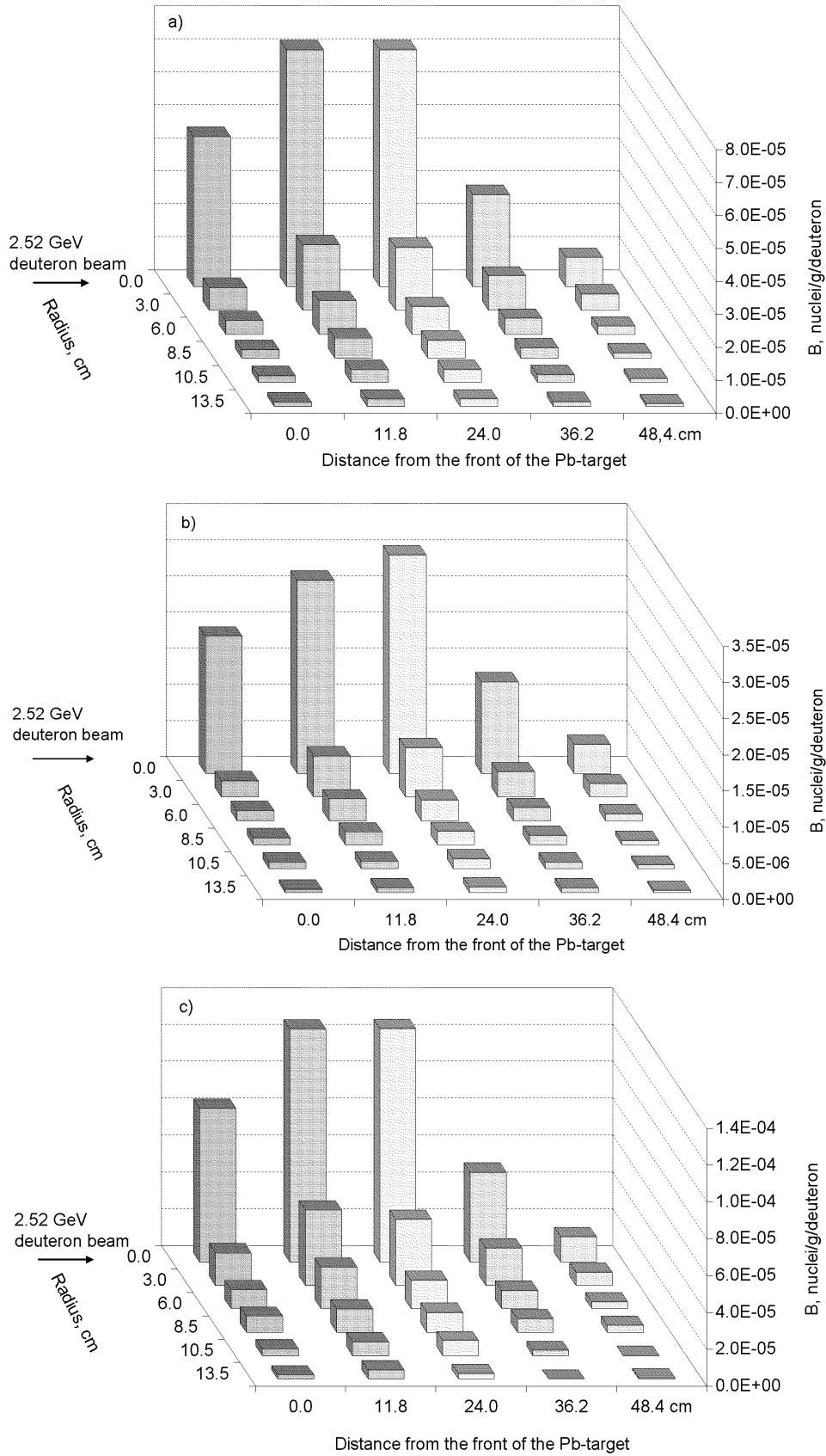


Fig. 10. Distributions of B-values $B(A_{res})$ for isotopes ^{88}Y (a), ^{87}Y (b) and ^{86}Y (c) produced in Y-foils by (n,2n), (n,3n), and (n,4n) reactions with threshold energies 11.5 MeV, 20.8 MeV and 32.7 MeV, respectively

Table 6. $B(A_{res}) \cdot 10^5$ – values for products observed in ^{89}Y detectors positioned at 0.0 cm, 11.8 cm, 24.0 cm, 36.2 cm and 48.4 cm from the front of the Pb-target (see Figs 1 and 6)

Residual nuclei, $T_{1/2}$, γ -lines used	Radial distance, cm	Axial distance from front of Pb-target, cm				
		0.0	11.8	24.0	36.2	48.4
^{88}Y $T_{1/2} = 106.65$ d, $E\gamma = 898.0$ and 1836.0 keV	0.0	8.34 (6)	12.7 (4)	12.7 (17)	4.874 (12)	1.37 (5)
	3.0	1.77 (11)	4.1 (4)	3.58 (12)	2.04 (13)	0.70 (8)
	6.0	1.03 (10)	2.25 (8)	1.56 (3)	0.997 (2)	0.38 (12)
	8.5	0.87 (20)	1.26 (5)	1.075 (2)	0.741 (9)	0.373 (5)
	10.5	0.38 (11)	0.74 (17)	0.82 (3)	0.285 (19)	–
	13.5	0.23 (5)	0.50 (4)	0.30 (10)	–	0.075 (6)
^{87}Y $T_{1/2} = 3.32$ d $E\gamma = 388.5$ and 484.8 keV	0.0	4.55 (5)	7.175 (13)	7.18 (4)	2.785 (8)	0.875 (8)
	3.0	0.694 (4)	1.988 (11)	1.899 (21)	1.048 (1)	0.509 (3)
	6.0	0.415 (10)	1.025 (5)	0.841 (3)	0.483 (5)	0.250 (3)
	8.5	0.264 (11)	0.611 (3)	0.540 (13)	0.323 (2)	0.158 (1)
	10.5	0.197 (4)	0.383 (7)	0.379 (9)	0.227 (7)	0.115 (10)
	13.5	0.126 (3)	0.216 (4)	0.211 (2)	0.141 (9)	0.074 (5)
^{86}Y $T_{1/2} = 0.614$ d $E\gamma = 1076.0$ keV	0.0	1.89 (13)	2.67 (10)	3.02 (15)	1.26 (8)	0.400 (27)
	3.0	0.224 (15)	0.57 (4)	0.69 (3)	0.350 (25)	0.184 (14)
	6.0	0.141 (17)	0.304 (22)	0.29 (3)	0.185 (17)	0.098 (13)
	8.5	0.100 (23)	0.174 (16)	0.184 (21)	0.126 (11)	0.057 (8)
	10.5	0.086 (19)	0.099 (10)	0.133 (16)	0.085 (15)	0.046 (10)
	13.5	0.042 (13)	0.060 (8)	0.075 (10)	0.060 (13)	0.026 (6)

Some general features of the experimental distributions are as follows:

There is a clearly defined maximum in yield around the distance $Z = 16 \pm 2$ cm from the front of the target.

The $B(A_{res})$ value is decreasing with increasing radial distance from the target axis (beam axis position) for those reactions that are induced by neutrons with energies above 5 MeV. The corresponding distributions show an almost exponential radial decrease.

The $B(A_{res})$ distribution for the non-threshold $^{197}\text{Au}(n,\gamma)^{198}\text{Au}$ reaction is almost flat.

One can conclude that the epithermal and resonance neutron flux (i.e., the “low energy flux”) is almost constant within the Pb-target whereas the flux of high energy neutrons strongly decreases with radial distance from the target axis. These features are very similar to previous experimental results obtained using proton beams.^{4,30,31}

Test measurements using a ^3He electronic neutron counter system

Before the start of the main deuteron irradiation short irradiations of emulsions and SSNT-detectors were made and simultaneously several neutron spectra using the ^3He electronic counter system were collected. Thermal neutrons were registered in the electronic system via the reaction $^3\text{He}(n,p)^3\text{H}$ having a Q -value of +764 keV. The energy of the emitted proton is electronically registered. In all measured spectra the proton peak at 764 keV from thermal neutrons is

distorted through pile-up which happened despite the low beam intensity, specifically lowered for these irradiations. As an example the spectra collected during the Polaroid exposure with only 1 pulse and during the irradiation for emulsions (6 pulses) are presented in Fig. 11. The count rate during these measurements was calculated to be in the range from 14 to 17 kcps. To prevent detector overload the counter was placed at a large distance from the Pb/U target behind the concrete shield (Fig. 4). The spectrum collected in this position during the entire irradiation lasting 7 hours is also presented in Fig. 11. The second peak seen in all spectra at about 1.5 MeV is a coincidence peak of two thermal neutrons. The count rate in all spectra actually exceeded the limit of this system for neutron spectrometry. Useful neutron spectra using this on-line neutron counting technique will need much lower beam intensities and longer extracted times for beam pulses.

Neutron distribution measurements using SSNT-detectors

The SSNT-detectors were used in the same way as in previous activation experiments.^{5–7}

The fast neutron distribution along the U-blanket: The neutron flux on the surface of the U-blanket reflects neutron production along the Pb-target from spallation reactions by primary and secondary particles and also the neutron production in the uranium blanket by secondary particles.

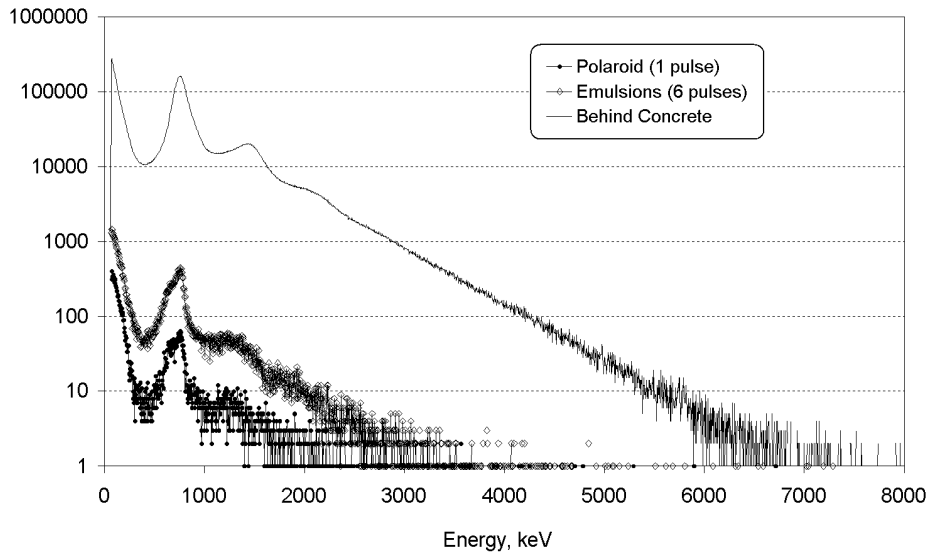


Fig. 11. Spectra collected with the ^3He counting system. The “bottom” and the “middle” spectra were accumulated with the ^3He detector using 1 and 6 pulses of the deuteron beam, respectively, in front of the concrete wall. The “top” spectrum shows the neutron spectrum collected with the same detector during 7 hours of main irradiation of the target, and placed at approx. 5.8 m distance behind the concrete wall (see Fig. 4)

Thermal neutrons were not detected in the target area because no difference between the tracks density on the Cd-covered and the Cd-uncovered regions of CR39 with $\text{Li}_2\text{B}_4\text{O}_7$ converter was observed. The same conclusion was verified by the supplementary measurements of thermal neutrons using ^{235}U fission detectors.³² The track density of the Cd-covered region of the CR39 detector with $\text{Li}_2\text{B}_4\text{O}_7$ converter corresponds to a fluence of epithermal neutrons (up to 10 keV) which is one order of magnitude lower than the fast neutrons fluence (between 0.3 and 3 MeV) which is detected by proton recoil on the bare CR39 detector. Thus it is obvious that the U/Pb-assembly produces mostly epithermal and fast neutrons.

Fission detectors with ^{232}Th -samples were used to measure the fast neutron flux above 2 MeV. The fast neutron intensity along the U-blanket is one order of magnitude smaller than the fluence of neutrons in the energy range (0.3–3) MeV measured with CR39. The results are shown in Fig. 12. Similar intensities of the neutron fluence were calculated with the high-energy transport code DCM-DEM (Dubna).³³ The fast neutron production increases until about 15 cm from the beam entrance and then decreases along the target. A similar intensity distribution and about the same intensities of fast neutrons had been determined in the same target arrangement irradiated by a 1.5 GeV proton beam.⁵

The fluence of thermal and fast neutrons escaping the shielding was also measured with CR39 detectors. The intensity of fast neutrons escaping the polyethylene shielding was two orders of magnitude lower than on the surface of the U-blanket (Fig. 13). The polyethylene shielding is an efficient moderator thermalizing a large fraction of the fast neutrons produced inside the U/Pb-assembly.

The spatial and energy distribution of neutrons: In this part measured results of fission rate distributions of ^{238}U and ^{235}U , capture reactions of neutrons by ^{238}U , and also the spectral index $\frac{\bar{\sigma}_{\text{capt}}^{238\text{U}}}{\bar{\sigma}_{\text{fiss}}^{238\text{U}}}$ at various radial positions on the U/Pb-assembly are presented. The comparison of the experimental data with results of calculations using model programs for simulation on the basis of Monte Carlo methods is also given. One of the primary goals was the development of a technique for measurements of the spectral index. This technique allows the determination of the spatial distribution of ^{239}Pu accumulation in the ^{238}U -blanket as a result of neutron capture reactions by ^{238}U . The spectral index is defined as the ratio of the number of capture reactions to the number of fissions in the U-blanket material. Results of measurements and calculations of axial and radial distributions of ^{238}U (n, γ) neutron capture reactions are given in Fig. 14.

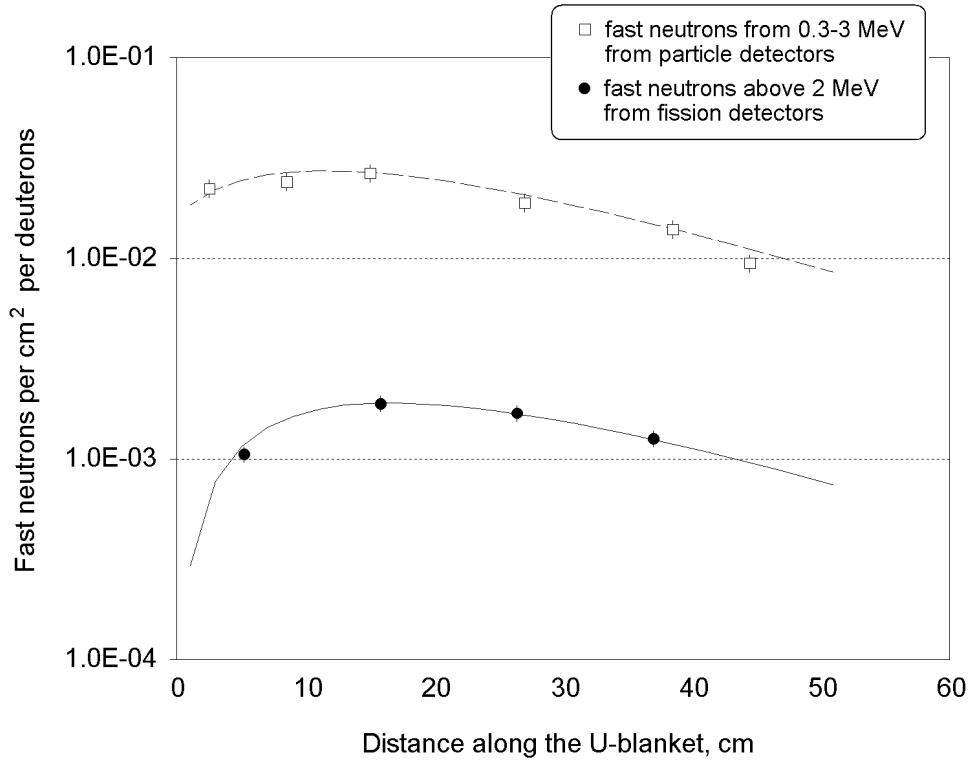


Fig. 12. The fast neutron distributions along the U-blanket measured with particle- and fission-detectors. Fast neutrons from 0.3 up to 3 MeV were measured with CR39 particle track detectors. Fast neutrons above 2 MeV are measured with Th-samples in contact with fission fragment detectors

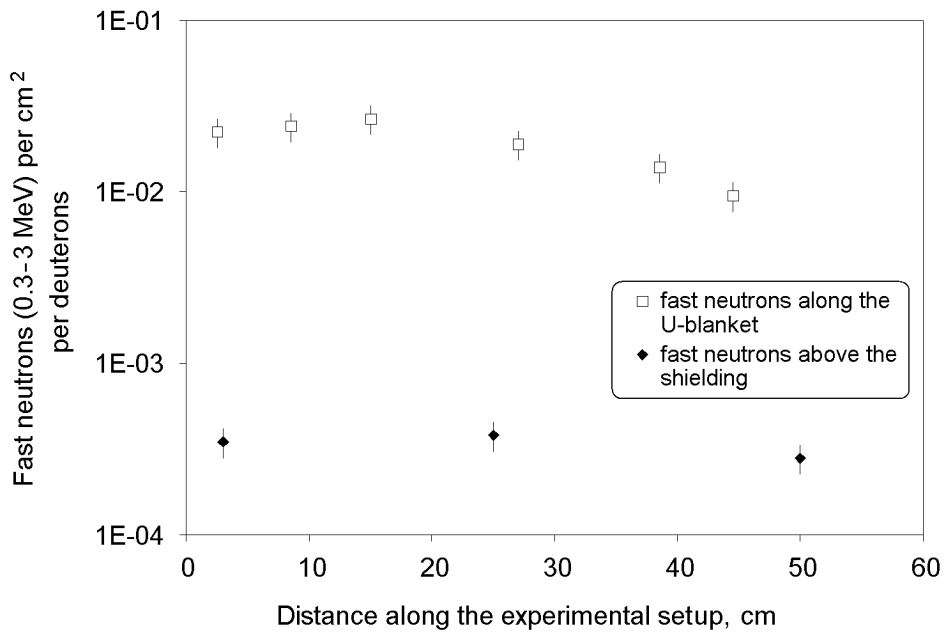


Fig. 13. Intensity distribution of fast neutrons escaping the polyethylene shielding and comparison with the distribution along the top surface of the U-blanket. Both distributions are measured with CR39 particle track detectors

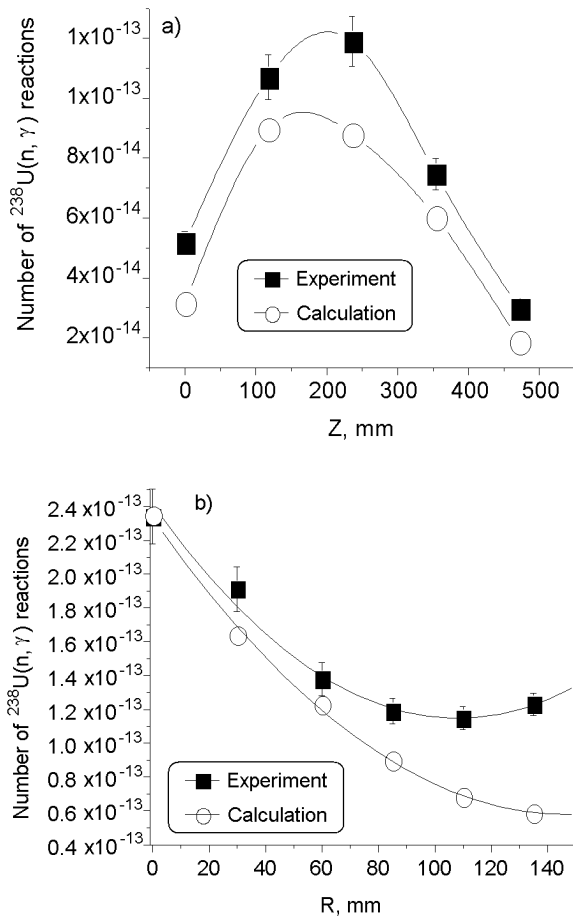


Fig. 14. Number of $^{238}\text{U}(n, \gamma)$ neutron capture reactions per one atom of ^{238}U and one incident deuteron; (a) longitudinal distribution along the uranium blanket (at radial distance $R = 85$ mm from the beam axis of the assembly); (b) radial distribution (at longitudinal distance $Z = 118$ mm from the target front). Lines are drawn to guide the eye

It can be seen from Fig. 14a that the results of measurements and the calculation of reaction rates of neutron capture of ^{238}U in the center of the blanket differ by over 30%. In radial direction (Fig. 14b) the cross section of the $^{238}\text{U}(n, \gamma)$ neutron capture reaction decreases with distance from the Pb-target axis. Experimental results at distances over 60 mm from the axis of the assembly are of special interest for comparison with the calculations by various codes, as significant deviations from the experiment are encountered. The experimental reaction rate exceeds the calculation by a factor of over 2. This significant difference may possibly be explained by the influence of neutrons slowed down and reflected by the biological shield.

Knowing the yield of the fission products³⁴ it is possible to determine the fission probability distribution

of ^{238}U . In this context, inter-comparison of results from measurements using two independent experimental methods (i.e., activation method and SSNTD) as well as comparison with calculated results is of high interest.

It is obvious from Fig. 15a that radial distributions of ^{238}U fission rates determined by two experimental methods coincide within the experimental uncertainties at distances larger than 30 mm from the Pb-target axis. Calculations also describe the fission process in the blanket material (natural uranium) and on the periphery of the assembly very well.

Results for the experimental and calculated values of spectral indices coincide within limits of experimental uncertainties up to a radial distance of $R = 120$ mm (Fig. 16). An increase of about 50% is observed at $R > 120$ mm in the periphery of the assembly. This shows an underestimation in calculations of the possible influence of neutrons moderated in and reflected by the biological shielding.

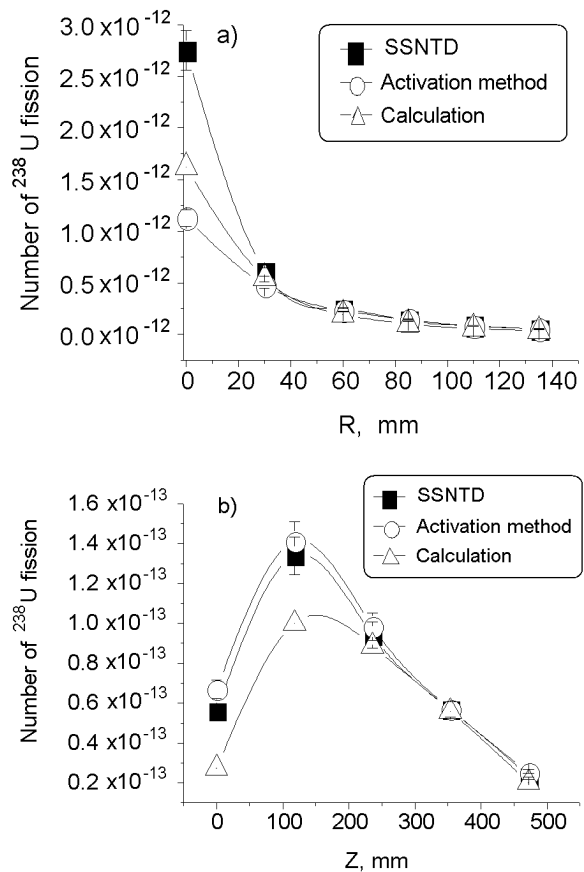


Fig. 15. Number of neutron induced fission reactions $^{238}\text{U}(n, f)$ per one atom of ^{238}U and one incident deuteron; (a) radial distribution at longitudinal distance $Z = 118$ mm and (b) axial distribution at radial distance $R = 85$ mm from the beam axis. Lines are drawn to guide the eyes

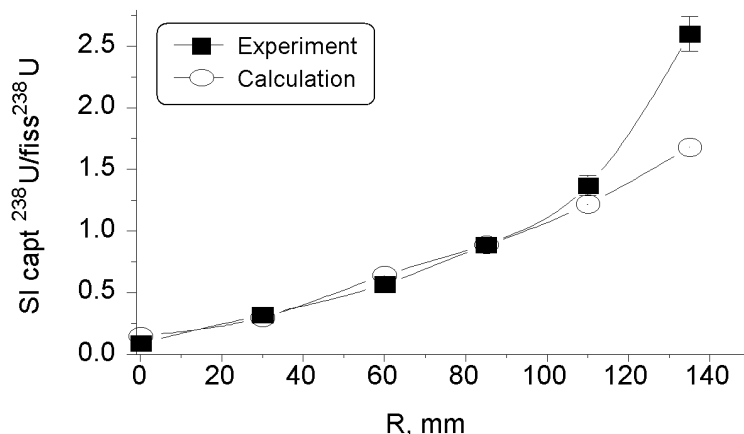
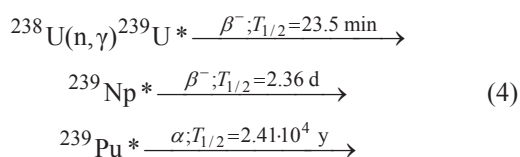


Fig. 16. Radial distribution of the spectral index $\text{SI} [^{238}\text{U}(n,\gamma)/^{238}\text{U}(n,\text{fiss})]$ in the first gap at longitudinal distance $Z = 118$ mm from the Pb-target front. Lines are drawn to guide the eyes

It is seen from Fig. 16 that the number of fissions of ^{238}U in the blanket exceeds the number of captured neutrons by a factor of three for $R < 32$ mm which is the border between the lead target and the U-blanket. Neutron capture then begins to prevail with increasing radial distance, probably because neutrons are moderated by collisions in the blanket material and by back-diffusion of epithermal neutrons from the polyethylene shield.

The procedure of combining the track counting and gamma-spectrometry techniques for the determination of spectral indices is a new development. It involves gathering information from the same sample by SSNTD-methods, i.e., counting the fission tracks of ^{238}U , and also by γ -ray spectrometry, i.e., counting a γ -line from the nuclide ^{239}Np at 277.6 keV:



This novel method allows the measurement of the spectral index with an uncertainty no more than $\pm 15\%$. It also allows quantitative determination of ^{239}Pu -accumulation in the $^{\text{nat}}\text{U}$ -blanket. Experimental value of the total mass of ^{239}Pu accumulated in the blanket is $(1.6 \pm 0.2) \cdot 10^{-8}$ g during the experiment, which compares well with the calculated value of $1.43 \cdot 10^{-8}$ g using the MCNPX code.³⁵ The MCNPX code was used and described in the literature quite often, for example in Reference 9.

Conclusions

We performed the first experiment to investigate transmutation (incineration) of radioactive waste from nuclear reactors (^{129}I , ^{237}Np , ^{238}Pu and ^{239}Pu) using a deuteron beam with 2.52 GeV kinetic energy. Neutron spatial distribution measurements were performed along the spallation source which consists of the Pb-target surrounded by U-blanket. Neutron distributions were studied using activation threshold detectors and solid state nuclear track detectors (SSNTD). The spallation neutron source provided very high fluxes of fast neutrons. The epithermal neutron flux is one order of magnitude less intense than the flux of fast neutrons. The intensity of thermal neutrons is negligible. The fast neutron distribution along the uranium blanket surface show an increase in intensity up to about 15 cm after beam entrance into the Pb-target and then a decrease along the target.

For the first time in our investigations on accelerator driven systems (ADS) He-3 electronic counters were tested in order to determine the neutron spectra.

Natural uranium foils were used to measure the (n,γ) reaction rates along the target length and in radial direction. Spectral indices (i.e., capture to fission ratios) were also determined. Experimental results were compared with MCNPX simulations. Experimental and simulated values of spectral indices agree well. The total experimental value of the ^{239}Pu production in the entire $^{\text{nat}}\text{U}$ -blanket during this deuterium irradiation was estimated from samples as $(1.6 \pm 0.2) \cdot 10^{-8}$ g ^{239}Pu , the calculated value using the MCNPX code is $1.43 \cdot 10^{-8}$ g ^{239}Pu .

This experiment is a continuation of investigations on this extended $^{\text{nat}}\text{U}/\text{Pb}$ -assembly in irradiations with protons of energies between 0.7 and 2.0 GeV.²⁻¹¹

*

The authors are grateful to Professors V. G. KADYSHEVSKY, A. N. SISSAKIAN, G. D. SHIRKOV, S. VOKAL and N. N. AGAPOV for their support of transmutation studies and to Drs. Yu. S. ANISIMOV, S. V. AFANASEV and P. I. ZARUBIN for their support of preparation and realization of the experiments using Nuclotron beams on the “Energy plus Transmutation” setup.

We thank the technical personnel of the Laboratory of High Energies JINR for providing effective operation of the accelerator during the irradiations of the lead target with uranium blanket.

Authors are grateful to members of Joint scientific seminar of Laboratory of High Energies and Laboratory of Physics Particles JINR (Scientific Leader of Seminar Professor V. A. NIKITIN) for useful constructive discussions about the results of this experiment.

Authors are grateful to the Agency of Atomic Energy of the Russian Federation for providing the material to build the uranium blanket, the main part of the experimental installation “Energy plus Transmutation” and to the JINR Directorate, who provided the operation of the accelerator facility.

This work was partly supported by the Czech Committee for the collaboration with laboratories of JINR GACR (202/03/4043) and project Open Science and Poland Committee for the collaboration with the laboratories of JINR. The work was partly supported by the Bulgarian Science Foundation (Contract Ph. 1311) and Project CECO. The authors would like to thank D. K. DRYABLOV (Laboratory of High Energies JINR) and S. M. KRIVOPUSTOV (International University of Nature, Society and Mankind “Dubna”) for technical help in preparing this publication.

One of the authors (M.I.K.) is grateful to the Directorate of the Institute of Nuclear Physics (Řež near Praha, Czech Republic) for creating favorable conditions on the last stage of preparation of this publication.

References

1. M. I. KRIVOPUSTOV, D. CHULTEM, TS. TUMENDELGER, Modeling of the Electronuclear Method of Energy Production and Study of Radioactive Waste Transmutation Using a Proton Beam of the JINR Synchrophasotron/Nuclotron, in: Research Program of the Laboratory of High Energies, A. M. BALDIN (Ed.) JINR-Communication 99-266, Dubna, Russia, 1999, p. 135.
- 2a. M. I. KRIVOPUSTOV, D. CHULTEM, J. ADAM, M. P. BELYAKOVA, V. G. KALINNIKOV, L. A. LOMOVA, A. V. PAVLIOUK, V. P. PERELYGIN, A. POLANSKI, E. B. SADOVSKAYA, A. N. SOSNIN, ZH. SERETER, TS. TUMENDELGER, SH. GERBISH, ZH. GANZORIG, P. S. KAZNOVSKI, S. P. KASNOVSKI, S. G. LOBANOV, V. F. MISCHENKOV, B. I. FONAREV, YU. L. SHAPOVALOV, R. ODOJ, A. M. KHEILMANOVICH, B. A. MARTSINKEVICH, S. V. KORNEEV, E.-J. LANGROCK, I. V. ZHUK, M. K. KIEVITS, E. M. LOMONOSOVA, R. BRANDT, W. WESTMEIER, H. ROBOTHAM, M. BIELEVICZ, A. VOJCECHOWSKI, Z. STRUGALSKI, V. WAGNER, A. KUGLER, S. R. HASHEMI-NEZHAD, M. ZAMANI-VALASIADOU, J. ADLOFF, M. DEBEAUVAIS, On a First Experiment on the Calorimetry of an Uranium Blanket Using the Model of the U/Pb Electro-Nuclear Assembly “Energy plus Transmutation” on a 1.5 GeV Proton Beam from the Dubna Synchrophasotron, JINR – Preprint P1 – 2000 – 168, Dubna, 2000 (in Russian).
- 2b. M. I. KRIVOPUSTOV, D. CHULTEM, J. ADAM, V. G. KALINNIKOV, A. V. PAVLIOUK, V. P. PERELYGIN, A. POLANSKI, A. N. SOSNIN, ZH. SERETER, O. S. ZAVERIYUKHA, TS. TUMENDELGER, SH. GERBISH, ZH. GANZORIG, P. S. KAZNOVSKI, S. P. KASNOVSKI, S. G. LOBANOV, V. F. MISCHENKOV, B. I. FONAREV, YU. L. SHAPOVALOV, R. ODOJ, S. E. CHIGRINOV, A. M. KHEILMANOVICH, M. K. KIEVITS, S. V. KORNEEV, E. M. LOMONOSOVA, A. MARTSINKEVICH, I. V. ZHUK, E.-J. LANGROCK, A. V. VORONKOV, R. BRANDT, H. ROBOTHAM, P. VATER, W. WESTMEIER, M. BIELEVICZ, M. SHUTA, Z. STRUGALSKI, A. VOJCECHOWSKI, A. KUGLER, V. WAGNER, S. R. HASHEMI-NEZHAD, M. ZAMANI-VALASIADOU, J. ADLOFF, M. DEBEAUVAIS, K. K. DWIVEDI, Kerntechnik, 68 (2003) 48.
3. J.-S. WAN, E.-J. LANGROCK, W. WESTMEIER, P. VATER, R. BRANDT, J. ADAM, V. BRADNOVA, A. BALABEKIAN, V. G. KALINNIKOV, V. S. PRONSKIKH, A. A. SOLNYSKHIN, V. I. STEGAILOV, V. M. TSOUPOKO-SITNIKOVA, B. A. KULAKOV, M. I. KRIVOPUSTOV, A. N. SOSNIN, G. MODOLO, R. ODOJ, S. R. HASHEMI-NEZHAD, M. ZAMANI-VALASIADOU, J. Radioanal. Nucl. Chem., 247 (2001) 151.
4. M. I. KRIVOPUSTOV, J. ADAM, A. R. BALABEKYAN, YU. A. BATUSOV, M. BIELEVICZ, R. BRANDT, P. CALOUN, D. CHULTEM, A. F. ELISHEV, M. FRAGOPOULOU, S. R. HASHEMI-NEZHAD, V. HENZL, D. HENZLOVA, V. G. KALINNIKOV, M. K. KIEVITS, A. KRÁSA, F. KRÍŽEK, A. KUGLER, M. MANOLOPOULOU, I. I. MARIIN, R. ODOJ, A. V. PAVLYUK, V. S. PRONSKIKH, H. ROBOTHAM, K. SIEMON, M. SZUTA, V. I. STEGAILOV, A. A. SOLNYSKHIN, A. N. SOSNIN, S. STOULOS, V. M. TSOUPOKO-SITNIKOVA, TS. TUMENDELGER, A. VOJCECHOWSKI, V. WAGNER, W. WESTMEIER, M. ZAMANI-VALASIADOU, O. S. ZAVERIYUKHA, I. V. ZHUK, Investigation of Neutron Spectra and Transmutation Studies of ^{129}I , ^{237}Np and Other Nuclides with 1.5 GeV Protons from the Nuclotron, JINR Preprint E1-2004-79, Dubna, Russia, 2004, Submitted to Nucl. Instr. Meth. in Phys. Res. A.
5. M. ZAMANI, M. FRAGOPOULOU, M. MANOLOPOULOU, S. STOULOS, A. SPYROU, M. DEBEAUVAIS, R. BRANDT, W. WESTMEIER, M. I. KRIVOPUSTOV, A. N. SOSNIN, Nucl. Instr. Meth. Phys. Res., A504 (2003) 454.
6. S. STOULOS, M. FRAGOPOULOU, J. C. ADLOFF, M. DEBEAUVAIS, R. BRANDT, W. WESTMEIER, M. I. KRIVOPUSTOV, A. N. SOSNIN, C. PASTEFANOU, M. ZAMANI, M. MANOLOPOULOU, Appl. Radiation Isotopes, 58 (2003) 169.
7. I. V. ZHUK, M. K. KIEVITS, M. I. KRIVOPUSTOV, A. N. SOSNIN, D. CHULTEM, W. WESTMEIER, H. ROBOTHAM, R. BRANDT, TS. TUMENDELGER, A. V. PAVLYUK, O. S. ZAVERIYUKHA, Investigation of Space and Energy Distribution of Neutrons in the Lead Target and the Uranium Blanket of the Electronuclear Installation “Energy plus Transmutation” During Irradiation with Proton at 1.5 GeV, JINR-Preprint R1-2002-84, Dubna, Russia, 2002 and Vesti NAN Belarus (Series Physics and Mathematics), Minsk, 12 (2003) 31.
8. B. A. MARCYNKEVICH, A. M. KHEILMANOVICH, S. V. KORNEEV, I. L. RAKHNOV, S. E. CHIGRINOV, M. I. KRIVOPUSTOV, A. N. SOSNIN, D. CHULTEM, TS. TUMENDELGER, A. V. PAVLYUK, O. S. ZAVERIYUKHA, Unfolding of Fast Neutron Spectra in the Wide Energy Range (up to 200 MeV) in a Heterogeneous Subcritical Assembly of an Electronuclear System “Energy plus Transmutation”, JINR – Preprint R1-2002-65, Dubna, Russia, 2002 and Vesti NAN Belarus (Series Physics and Mathematics), Minsk, 1 (2004) 90.
9. S. R. HASHEMI-NEZHAD, R. BRANDT, W. WESTMEIER, R. ODOJ, KH. M. HELLA, M. I. KRIVOPUSTOV, B. A. KULAKOV, A. N. SOSNIN, Radiat. Meas., 36 (2003) 295.

10. M. I. KRIVOPUSTOV, J. ADAM, V. BRADNOVA, R. BRANDT, V. S. BUTSEV, P. I. GOLUBEV, V. G. KALINNIKOV, B. A. KULAKOV, E.-J. LANGROCK, G. MODOLO, M. OCHS, R. ODOJ, A. N. PREMYSHEV, V. I. STEGAILOV, J. S. WAN, V. M. TSOUPOKO-SITNIKOVA, *J. Radioanal. Nucl. Chem.*, 222 (1997) 267.
11. J. S. WAN, M. OCHS, I. G. ABDULLAEV, J. ADAM, J. C. ADLOFF, V. P. BAMBLEVSKIY, V. BRADNOVA, R. BRANDT, V. S. BUTSEV, M. DEBEAUVAIS, K. K. DWIVEDI, L. GELOVANI, P. I. GOLUBEV, V. K. KALINNIKOV, J. KARACHUK, M. I. KRIVOPUSTOV, B. A. KULAKOV, E.-J. LANGROCK, G. MODOLO, R. ODOJ, V. P. PERELYGIN, P.-W. PHILIPPEN, A. N. PREMYSHEV, V. S. PRONSKICH, A. N. SOSNIN, V. I. STEGAILOV, B. WILSON, M. ZAMANI, V. M. TSOUPOKO-SITNIKOVA, *Kerntechnik*, 63 (1998) 167.
12. A. M. BALDIN, A. I. MALAKHOV, A. N. SISSAKIAN, *Problems of Relativistic Nuclear Physics and Multiple Particle Production*. JINR-Communication R1-2001-106, Dubna, Russia, 2001, p. 55, and *Physics of Particles and Nuclei*, 32 Suppl. 1 (2001) 4.
13. A. I. MALAKHOV, A. N. SISSAKIAN, A. S. SORIN, S. VOKAL, *Relativistic Nuclear Physics at the Joint Institute for Nuclear Research*, JINR – Preprint R1-2006-93, Dubna, Russia, 2006, p. 60.
14. A. D. KOVALENKO, A. M. BALDIN, A. I. MALAKHOV, *Status of the Nuclotron*, Proc. EPAC-94, Vol. 1, June 1994, London, 1995, p. 161 and *Cryogenic system of the Nuclotron – A new superconducting synchrotron*, *Adv. Cryogen. Eng.*, 39 (1994) 501 and *Main Results and Development Plans*, *At. Energy*, 93 (2002) 479 (in Russian).
15. C. D. BOWMAN, E. D. ARTHUR, P. W. LISOWSKI, G. P. LAWRENCE, R. J. JENSEN, J. L. ANDERSON, B. BLIND, M. CAPIELLÒ, W. DAVIDSON, R. R. ENGLAND, L. N. ENGEL, R. C. HAIGHT, H. G. HUGHES, J. R. IRELAND, R. A. KRAKOWSKI, R. J. LABAUVE, B. C. LETELLIER, R. T. PERRY, G. J. RUSSEL, K. P. STAUDHAMMER, G. VERSAMIS, W. B. WILSON, *Nucl. Instr. Meth. Phys. Res.*, A320 (1992) 336.
16. C. RUBBIA, J. A. RUBIO, S. BUONO, F. CARMINATI, N. FIÉTIER, J. GÁLVEZ, C. GELÈS, Y. KADI, R. KLAPISCH, P. MANDRILLON, J. P. C. REVOL, C. ROCHE, *Conceptual Design of a Fast Neutron Operated High Power Energy Amplifier*, Report CERN-AT-95-44, September 20, 1995, Geneva, Switzerland.
17. H. NIFENECKER, S. DAVID, J. M. LOISEAUX, A. GIORNI, *Progr. Particle Nucl. Phys.*, 43 (1999) 683.
18. C. RUBBIA, *The Technical Working Group on ADS, A European Roadmap for Developing Accelerator Driven Systems (ADS) for Nuclear Waste Incineration*, ENEA 2001, ISBN 88-8286-008-6.
19. A. ABÁNADES, J. ALEXANDRE, S. ANDRIAMONJE, A. ANGELOPOULOS, A. APOSTOLAKIS, H. ARNOULD, E. BELLE, C. A. BOMPAS, D. BROZZI, J. BUENO, S. BUONO, F. CARMINATI, F. CASAGRANDE, P. CENNINI, J. I. COLLAR, E. CERRO, R. DEL MORAL, S. DIEZ, L. DUMPS, C. ELEFTHERIADIS, M. EMBID, R. FERNÁNDEZ, J. GÁLVEZ, J. GARCIA, C. GELÈS, A. GIORNI, E. GONZÁLEZ, O. GONZÁLEZ, I. GOULAS, D. HEUER, M. HUSSONNOIS, Y. KADI, P. KARAIKOS, G. KITIS, R. KLAPISCH, P. KOKKAS, V. LACOSTE, C. LE NAOUR, C. LÓPEZ, J. M. LOISEAUX, J. M. MARINEZ-VAL, O. MÉPLAN, H. NIFENECKER, J. OROPESA, I. PAPADOPOULOS, P. PAVLOPOULOS, E. PÉREZ-ENCISO, A. PÉREZ-NAVARRO, M. PERLADO, A. PLACCI, M. POZA, J.-P. REVOL, C. RUBBIA, J. A. RUBIO, L. SAKELLIIOU, F. SALDAÑA, E. SAVVIDIS, F. SCHUSSLER, C. SIRVENT, J. TAMARIT, D. TRUBERT, A. TZIMA, J. B. VIANO, S. VIEIRA, V. VLACHOUDIS, K. ZIOUTAS, *Results from the TARC Experiment: Spallation Neutron Phenomenology in Lead and Neutron-Driven Nuclear Transmutation by Adiabatic Resonance Crossing*, *Nucl. Instr. Meth. Phys. Res.*, A478 (2002) 577.
20. R. BRANDT, W. BIRKHOLZ, I. A. SHELAEV, *Kerntechnik*, 69 (2004) 37.
21. V. A. VORONKO, V. M. D'YACHENKO, V. YA. KOSTIN, L. G. LEVCHUK, V. S. IROSHNIK, V. YA. MIGALENYA, K. D. TOLSTOV, N. A. KHIZNYAK, *At. Energy*, 68 (1990) No. 6 and *Energy Generation of Neutrons in Light Nuclei in Lead Slot*, *JINR-Communication*, 2(53), Dubna, 1992, p. 17.
22. R. G. VASSIL'KOV, V. I. GOL'DANSKII, V. V. ORLOV, *Atomic Energy*, 29 (1970) 151 (in Russian) and *Success Phys. Sci.*, 139 (1983) 435 and *At. Energy*, 79 (1995) 257 (in Russian).
23. S. STOULOS, M. FRAGOPOULOU, M. MANOLOPOULOU, A. N. SOSNIN, M. I. KRIVOPUSTOV, W. WESTMEIER, R. BRANDT, M. DEBEAUVAIS, M. ZAMANI, *Nucl. Instr. Meth. Phys. Res.*, A519 (2004) 651.
24. J. R. HARVEY, R. J. TANNER, W. G. ARBERT, D. T. BARTLETT, E. K. PRESCH, H. SCHWEBE, *Radiat. Prot. Dosim.*, 77 (1998) 267.
25. M. MANOLOPOULOU, M. FRAGOPOULOU, S. STOULOS, C. KOUKORAVA, A. SPYROU, G. PERDIKAKIS, S. R. HASHEMI-NEZHAD, M. ZAMANI, *Nucl. Instr. Meth. Phys. Res.*, A562 (2006) 371.
26. J. FRÁNA, *J. Radioanal. Nucl. Chem.*, 257 (2003) 583.
27. J. BANAGS, J. BERGER, J. DUFLO, L. GOLDZAHN, O. HARFF, M. COTTEREAU, F. LEFEBVRES, H. QUÉCHON, P. TARDY-JOUBERT, *Nucl. Instr. Meth.*, A95 (1971) 307.
28. J. ADAM, K. KATOVSKY, A. R. BALABEKIAN, A. A. SOLNYSHKIN, V. G. KALINNIKOV, V. I. STEGAILOV, V. M. TSOUPOKO-SITNIKOVA, S. G. STETSENKO, M. I. KRIVOPUSTOV, V. S. PRONSKIKH, N. M. VLADIMIROVA, H. KUMAWAT, *Transmutation of ^{129}I , ^{237}Np , ^{239}Pu and ^{241}Am Using Neutrons Produced in Pb-target with ^{nat}U -blanket System "Energy plus Transmutation" Bombarded by 2.0 GeV Relativistic Protons*, Vol. 2, Proc. Intern. Conf. on Nuclear Data for Science and Technology, 26 September – 1 October, 2004, Santa Fe, New Mexico, USA, New York, 2005, p. 1560.
29. YU. E. TITARENKO, O. V. SHVEDOV, V. F. BATYAEV et al., *Nuclei Product Yields in ^{99}Tc Transmutation under 0.1–2.6 GeV Proton Bombardment*, Proc. Intern. Conf. on Subcritical Accelerator Driven Systems, 11–15 October, 1999, Moscow, Russia, 1999, p. 204.
30. M. BIELEVICH, M. SZUTA, A. WOJCIECHOWSKI, E. GOLA-STRUGALSKA, M. I. KRIVOPUSTOV, J. ADAM, A. KUGLER, V. WAGNER, A. KRASA, M. MAJERLE, P. CHALOUN, *On the Experiment of Neutron Spectrum Investigation on U/Pb-Assembly Using 0.7 GeV Proton Beam from the Nuclotron (Dubna)*, Proc. XVII Intern. Baldin Seminar on High Energy Physics Problems, Relativistic Nuclear Physics and Quantum Chromodynamics, Dubna, Vol. II, 27 September–2 October, 2004, Dubna, Russia, 2005, p. 125.
31. F. KRÍZEK, V. WAGNER, J. ADAM, P. CALOUN, V. HENZL, D. HENZLOVA, A. KRASA, A. KUGLER, M. MAJERLE, M. I. KRIVOPUSTOV, V. I. STEGAILOV, V. M. TSOUPOKO-SITNIKOVA, *Czech. J. Phys.*, 56 (2006) 243.
32. M. ZAMANI, M. FRAGOPOULOU, S. STOULOS, M. I. KRIVOPUSTOV, A. N. SOSNIN, R. BRANDT, W. WESTMEIER, M. MANOLOPOULOU, *A Spallation Neutron Source Based on Pb-target Surrounded by U-blanket*. (2006) Submitted to *Radiat. Meas.*
33. A. POLANSKI, A. N. SOSNIN, V. D. TONEEV, *JINR Preprint E2-91-562*, Dubna, 1991.
34. V. M. GORBACHEV, YU. S. ZAMYATIN, A. A. LBOV, *Interaction Ray with Heavy Element and Fission Nuclei*, Moscow, Atomizdat, 1978.
35. L. W. HENDRICKS, G. W. MCKINNEY, L. S. WATERS, *MCNPX, VERSION 2.5.e*, Report No. LA-UR-04-0569, Los Alamos National Laboratory, USA, February 2004.
36. U. REUS, W. WESTMEIER, *Catalog of Gamma-Rays from Radioactive Decay*, Atomic Data and Nuclear Data Tables, 29 (1983) Nos 1 and 2.